Comparative Analysis of PSF Estimation Based on Hough Transform and Radon Transform

Mayana Shah[1(✉)] and Upena Dalal[2]

[1] CKPCET, Surat, India
mayna.shah@ckpcet.ac.in
[2] SVNIT, Surat, India
udd@eced.svnit.ac.in

Abstract. Blind image motion deblurring (BID) is in great demand to recover the original image from its degraded observation. Motion blur is the effect of relative movement between camera and object during shutter opening. Restoring the information requires estimation of Point spread function (PSF) and use this PSF for deblurring task. PSF estimation plays important role in motion deblurring and mis-specification of kernel can lead to structural distortion in deblurred image. In this paper, we have proposed the comparative analysis of PSF estimation methods in modified cepstrum domain based on Hough transform and Radon transform. Experimentation is done on standard image and estimated parameters are compared for motion blur of different length and degrees. Conclusions are drawn on the basis of simulation study on Matlab for standard image.

Keywords: Image deblurring · Image restoration · Motion blur
PSF estimation

1 Introduction

The BID is mainly useful in almost all imaging related applications as normally there is always a chance of camera shake during the photo capturing process. The Deblurring result accuracy depends on the accuracy of PSF estimation. Once the PSF is accurately estimated, non-blind deblurring is used to get restored image. In most of the research work blurring process can be modelled by convolution formula as [1]:

$$g(x, y) = h(x, y) * f(x, y) \tag{1}$$

Equation (1) show that $g(x, y)$ captured degraded image is nothing but convolution of pristine image f with degradation function h. Here (x, y) Indicates spatial coordinates and "*" is the convolution operation. There are diverse techniques for image deblurring with simultaneous or separate PSF estimation. Comprehensive overview of all techniques is given by Wang and Tao in [2]. Comparison of all such techniques are given in Table 1.

Z. Patel and S. Gupta (Eds.): ICFITT 2017, LNICST 220, pp. 86–96, 2018.
https://doi.org/10.1007/978-3-319-73712-6_9

Table 1. Comparison of image deblurring techniques with simultaneous or separate PSF estimation

Type	Functionality	Advantage and limitations
Statistical methods	MAP Variational Edge prediction	Convergence problem Produce good results if converge to right solution Slow Requires prior information Face problem in restoring image with multiple neighboring edges [3–7]
Regularization	Tihkhonov Total Variation Dictionary learning	Regularization parameter setting effect the solution, Trade-off between performance and complexity [8–10]
Parametric methods	Spectral Cepstrum Modified Cepstrum	Simpler approach - less computation [11–16, 23, 24]
Hardware based methods	Use of gyroscopes Coded shutter Coded aperture	Corrects the blur before information is recorded on the sensor Costly High quality [17–20]
Multi-channel image restoration	Dual Camera	For multi images we require precise registration Slow computation [21, 22]

Our method is a parametric approach which uses a mathematical model of a uniform motion blur kernel h expressed in terms of parameters length L and theta θ as [1]:

$$h(x, y, L, \theta) = \begin{cases} \frac{1}{L}, & if\ \sqrt{x^2 + y^2} \leq L/2, x/y = -\tan^{-1}\theta \\ 0, & \text{otherwise} \end{cases} \tag{2}$$

To remove the blurring effect the parameters length L and theta θ should be decided accurately. Spectral representation of a blur kernel h is a sinc function as motion blur is kind of rectangular function. Zeros of the Sinc function helps to find out length L and orientation of sinc is in perpendicular direction of motion. Existing methods use log-spectral representation [11, 12] and Cepstral domain representations [13–15] of the blurred input image to obtain blur kernel estimation, but it may lead to erroneous angle estimation because of no of parallel stripes in magnitude spectrum. So to thin out central lobe we use dual operated log spectrum termed as modified cepstrum defined as follows [16]:

$$C = \log\{|\mathscr{F}\{\log\{|\mathscr{F}(g(x, y))|\}\}|\} \tag{3}$$

Despande shown modified cepstrum [16] has potential clues to identify PSF resulted from thin line segment view of central thick stripe in spectrum of blur image. To find out the direction of line segment there are two approaches first one by Hough

transform and second one by Radon transform. In this paper, we have presented a comparison of both approaches and shown that Radon transform based technique produces superior results compare to Hough transform based method. Hough transform is flexible to find lines in images and one can easily represent broken lines as a joint line but at specific angles its performance degrades and accuracy decreases.

Comparison of these two major approaches over wide range of blur parameter variation needed to be explored and effort of such comparative analysis is done in paper. The rest of the paper is organized as follows: Sect. 2 describes Hough Transform based parameter estimation and results. Radon Transform based parameter estimation and results is presented in Sect. 3. The comparison is discussed in Sect. 4 and the conclusions are summed up in Sect. 5.

2 Hough Transform Based Parameter Estimation

Modified cepstrum represents thin line segment in direction of motion blur. To find out the direction of line segment there are two approaches first one by Hough transform and second one by Radon transform. In our previous work [23, 24] Hough transform based algorithm were discussed that has been summarized in Algorithm 1.

Algorithm 1

1. Obtain modified cepstrum from grayscale blurred image (Fig.1(d))
2. Extract fourth bit plane of modified cepstrum image and use canny edge detection for finding the line segment. (Fig.1(e) and Fig.1(f))
3. Apply Hough transform on step 2 image and find Motion blur angle is identified as 180- the peak in Hough transform
4. Step one image is grayscale transform by threshold value 0.6. and rotate it by negative value of estimated angle (Fig.1(g))
5. Step 5 image is converted to 1-D by averaging of columns. Twin peak pattern is obtained with center peak and two side peaks. Averaging distance from center peak to two side peak is considered as blur length. (Fig.1(h))

Results for cameraman image of size 256×256 is presented in Table 2 for degradation by different lengths ($5 \leq L \leq 80$) and different directions ($10 \leq \theta < 170$). Error equals to the estimated value minus the real value. The results are as shown in Fig. 1.

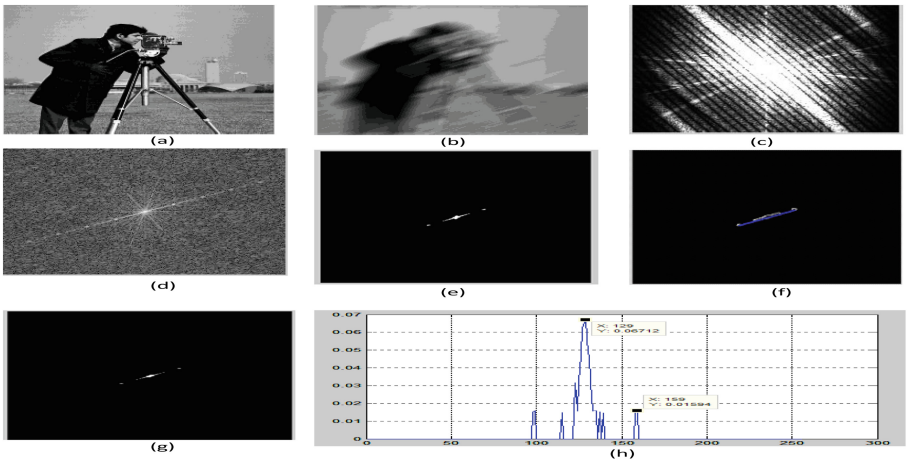

Fig. 1. Results of proposed algorithm for uniform blur without noise (a) original cameraman (b) blurred image with L = 30 pixels and θ = 30°, (c) log spectrum (d) modified cepstrum domain (e) thin line segment extracted from fourth bitplane of modified cepstrum (f) edge detection and Hough based angle estimation θ^ = 28° (g) grayscale transformation of modified cepstrum with threshold 0.6 (h) twin peak representation and blur length estimation L^ = 30

Based on Estimated parameters in Table 2 graph is plotted for true length Vs absolute error for various blur direction and result is shown in Fig. 2(a) and (b). From Fig. 2(a) and (b) it is observed that maximum error in blur length estimation is 1 pixel.

A result for Blur angle estimation for camera man image is given in Table 3. Based on Estimated parameters graph is plotted for true angle Vs absolute error for various blur length and result is shown in Fig. 3(a) and (b). Graphical representation shows that maximum error in blur angle estimation is 4°.

Table 2. Results for blur length estimation for cameraman image.

True L in *pixels*		5	10	15	20	25	30	35	40	45	50	55	60	65	70	75	80
		Estimated blur length															
Blur angle in degrees	10	5	10	15	20	25	30	35.5	40	45.5	50	55	60	65	70	75	80
	20	5.5	9.5	15	20	25	31	35	39.5	45	50	54.5	60	65	70	75.5	80
	30	5.5	10	15	19.5	25	30	35.5	40.5	45.5	50	55	60	65.5	70	75	80
	40	5	10.5	14.5	20	24.5	30	35	40	45	50.5	55.5	60.5	65	70	75	80
	50	5	10.5	15	20	25	30	35	40	45.5	50	55.5	60	64.5	70	75	80
	60	6	10.5	15	19.5	25	30	35.5	40	45.5	49.5	55	60	64.5	70	75	79.5
	70	5.5	9.5	15.5	20	25	30.5	35	40	45.5	50	54	60	66	69	75	80
	80	5	10	15	20	25	29.5	35.5	39.5	45.5	50	55.5	60	65	70	75	80
	90	5	10	15	20	25	30	35	40	45	50	55	60	65	70	75	80
	100	5	10	15	20	25	30	35.5	40	45.5	50	55	60	65	70	75	80
	110	5	9.5	15	20	25	30	35	39.5	45.5	50	54	60.5	65	69.5	75.5	79.5
	120	6	10	15	20	25	30	35	40	45	50.5	54.5	60	65	70.5	75	80
	130	5	10.5	15	20	25.5	30	35	40	45	50.5	54.5	60.5	65	69.5	75	80
	140	5	10	15	20	25.5	30	35	40	45.5	50.5	55	60.5	64.5	69.5	75.5	80
	150	5	10	15	19.5	25	30	35	40.5	45	50	54.5	60	65	70	74.5	79.5
	160	5	9.5	15	20	25	30	35	39.5	45.5	50	54.5	60.5	65	69.5	75.5	80
	170	5	10	15	20	25	30	35.5	40	45.5	50	55	60	65	70	75	80

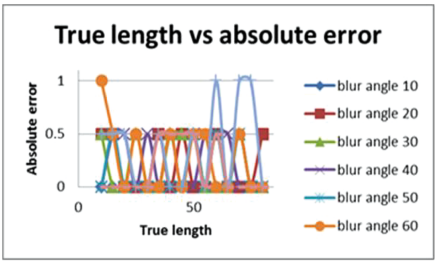

(a)

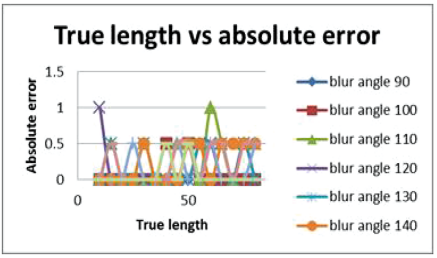

(b)

Fig. 2. (a) True length vs absolute error for blur angle variation 10° to 60° (b) True length vs absolute error for blur angle variation 90° to 140°

Table 3. Results for blur angle estimation for cameraman image.

L in *pixels*		10	15	20	25	30	35	40	45	50	55	60	65	70	75	80
		Estimated blur angle in degrees														
Blur angle in degrees	10	9	9	9	9	10	9	9	10	9	9	9	9	9	9	9
	20	19	20	19	19	19	19	19	19	19	19	19	19	19	19	19
	30	28	29	29	28	28	28	29	29	29	31	29	29	29	29	31
	40	44	44	44	39	39	44	39	39	39	39	39	39	39	39	39
	50	49	49	49	49	49	49	49	49	49	49	49	49	49	49	49
	60	60	60	60	60	60	60	59	59	59	60	60	59	60	59	60
	70	71	69	69	69	69	69	69	69	69	69	69	69	69	69	69
	80	79	79	78	79	79	79	79	78	79	79	79	79	79	79	79
	90	89	89	89	89	89	89	89	89	89	89	89	89	89	89	89
	100	97	99	99	99	99	99	99	99	99	99	99	99	99	99	99
	110	110	110	110	110	110	110	109	109	109	109	109	109	109	109	109
	120	119	119	119	119	119	119	119	119	119	119	119	119	119	119	119
	130	131	130	134	130	129	130	129	129	129	130	129	129	129	129	129
	140	137	138	137	139	137	138	139	138	139	139	139	139	139	139	139
	150	149	149	149	149	149	149	149	149	149	149	149	149	149	149	149
	160	159	159	159	159	159	158	159	159	159	159	159	159	159	159	159
	170	169	169	169	169	169	169	169	169	169	169	169	169	169	169	169

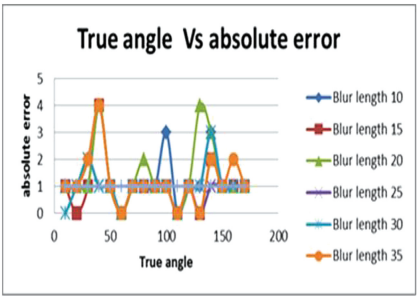

(a)

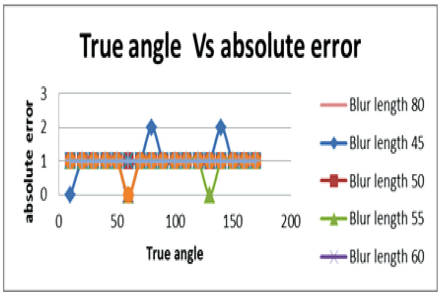

(b)

Fig. 3. (a) True angle vs absolute error for blur length 10 to 35 pixels (b) True angle vs absolute error for blur length 45 to 80 pixels

3 Radon Transform Based Parameter Estimation in Modified Cepstrum Domain

The Proposed scheme uses Radon Transform for blur direction identification. Radon Transform is kind of integral transform that computes the integration of a function along straight lines and useful to detect linear representations in images. Line in the modified cepstrum image will be represented by a peak in the Radon transform whose location determines the parameters of the line. Radon transform along this direction usually has larger variations so peak in radon transform corresponds to max value of variance. As the integration is along the perpendicular direction to a line, principal direction of motion blur is obtained by subtracting 90° from the max value of Radon transform. The detail method is discussed in Algorithm 2 and result is shown in Fig. 4.

Algoritham 2

1. Obtain modified cepstrum from grayscale blurred image (Fig.4(d))
2. Perform gray scale transformation on step 1 image with threshold=0.6 (Fig.4(e))
3. Find the principal direction using Radon transform as peak in Radon transform-90° (Fig.4(f)).
4. Rotate the grayscale transformed modified Cepstrum image of step 2 by negative value of estimated angle. (Fig.4(g))
5. Convert the 2-D matrix of step 4 to 1-D by taking the averages of columns. It will show a twin peak pattern. (Fig.4(h))
6. The distance between the central peak and first larger peak on either side is nothing but the estimated blur length in pixels (Fig.4(h)).

PSF estimation Algorithm 2 discussed is applied to Lena Image which was degraded by different lengths ($10 \leq L \leq 80$) and different directions ($10 \leq \theta° < 170$). The results are presented in Tables 4 and 5. Error equals to the estimated value minus the real value. The results are as shown in Fig. 4.

Based on Estimated parameters in Table 4 graph is plotted for true length Vs absolute error for various blur direction and result is shown in Fig. 5(a) and (b). It is observed that maximum error in blur length estimation is 1 pixel. A result for Blur angle estimation for Lena image of size 256×256 is given in Table 5. Based on Estimated parameters graph is plotted for true angle Vs absolute error for various blur length and result is shown in Fig. 6(a) and (b). Graphical representation shows that maximum error in blur angle estimation is 1°.

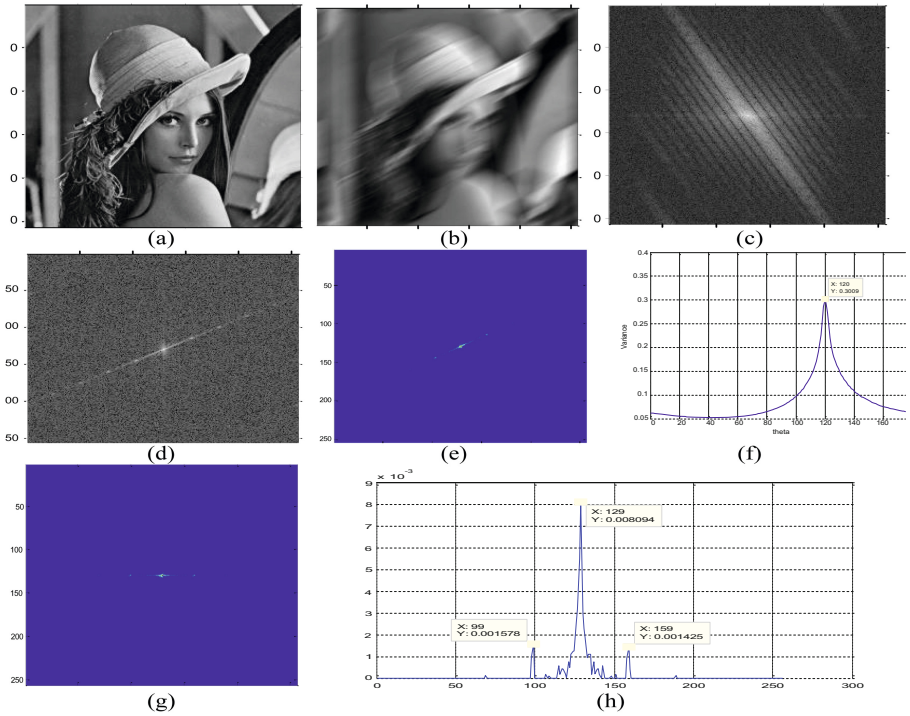

Fig. 4. Results of proposed algorithm for uniform blur (a) original Lena image (b) blurred image with L = 30 pixels and θ = 30°, (c) log spectrum (d) modified cepstrum domain (e) thin line segment extracted from Gray scale transform of modified cepstrum with threshold 0.6 (f) Radon transform based blur direction estimation θ^ = 30° (g) anticlockwise rotation of grayscale transformed modified cepstrum (h) twin peak representation and blur length L^ = 30 pixels

4 Comparison

Following observations can be made from experiments of Sects. 2 and 3:

- In case of Hough transform based blur angle estimation at specific angles such as 40° and 140° accuracy reduces and it shows maximum error of 4° and there are more chance of error for almost whole range of blur length.
- In case of Radon transform based blur length estimation accuracy is 87.45%. It shows great impact on deblurred image as deblurred image output quality is highly dependent on accuracy of PSF estimation in particular blur length.
- In case of Radon transform based blur angle estimation accuracy is 95.68% and most chance of error in blur angle measurement is in case where the blur length is lower or equal to ten. In case of Radon transform based blur angle estimation maximum error reduces to 1°.
- Almost zero error in blur angle estimation after blur length 15 pixels in Radon transform based approach.

Table 4. Results for blur length estimation for LENA 256 × 256 image

True L *in Pixels*		10	15	20	25	30	35	40	45	50	55	60	65	70	75	80
		Estimated blur length														
Blur angle 0°	10	10	15	20	25	30	36	40	46	50	55	60	65	70	75	80
	20	10	15	20	25	30	35	41	45	50	55	60	65	71	76	80
	30	10	15	20	25	30	36	40	45	50	55	60	65	70	75	80
	40	10	15	19	25	30	36	41	45	50	56	60	66	70	75	80
	50	10	15	20	25	30	35	40	45	50	56	60	65	70	75	80
	60	10	15	20	25	30	36	40	45	50	55	60	65	70	75	80
	70	10	15	20	25	30	34	41	45	49	54	59	64	71	74	81
	80	10	15	20	25	30	35	40	46	50	55	60	65	70	75	80
	90	10	15	20	25	30	35	40	45	50	55	60	65	70	75	80
	100	10	15	20	25	30	35	40	46	50	55	60	65	70	75	80
	110	10	15	20	26	30	35	40	46	50	55	60	64	69	76	81
	120	10	15	20	25	30	35	40	45	50	55	60	65	70	75	80
	130	10	14	20	25	30	35	40	45	50	55	60	65	70	75	80
	140	10	14	20	25	30	35	40	45	50	55	60	65	70	75	80
	150	10	15	20	25	30	35	40	45	50	55	60	65	70	75	80
	160	10	15	20	25	30	35	40	45	50	55	60	65	70	75	80
	170	10	15	20	25	30	35	40	45	50	55	60	65	70	75	80

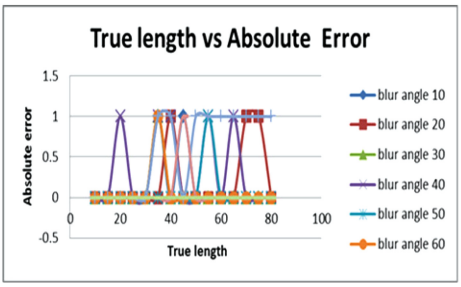

(a)

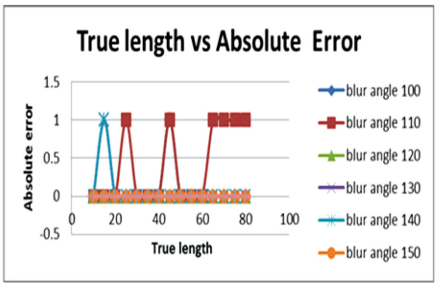

(b)

Fig. 5. (a) True length vs absolute error for blur angle 10° to 60° (b) True length vs absolute error for blur angle 100° to 150°

Table 5. Results for blur angle estimation for LENA 256 × 256 image.

L *in Pixels*		10	15	20	25	30	35	40	45	50	55	60	65	70	75	80
		Estimated blur angle														
Blur angle θ°	10	10	10	10	10	10	10	10	10	10	10	10	10	10	10	10
	20	21	20	20	20	20	20	20	20	20	20	20	20	20	20	20
	30	31	30	30	30	30	30	30	30	30	30	30	30	30	30	30
	40	40	40	40	40	40	40	40	40	40	40	40	40	40	40	40
	50	50	50	50	50	50	50	50	50	50	50	50	50	50	50	50
	60	61	60	60	60	60	60	60	60	60	60	60	60	60	60	60
	70	71	71	70	70	70	70	70	70	70	70	70	70	70	70	70
	80	79	80	80	80	80	80	80	80	80	80	80	80	80	80	80
	90	89	90	90	90	90	90	90	90	90	90	90	90	90	90	90
	100	101	100	100	100	100	100	100	100	100	100	100	100	100	100	100
	110	110	109	110	110	110	110	110	110	110	110	110	110	110	110	110
	120	119	120	120	120	120	120	120	120	120	120	120	120	120	120	120
	130	130	130	130	130	130	130	130	130	130	130	130	130	130	130	130
	140	139	140	140	140	140	140	140	140	140	140	140	140	140	140	140
	150	150	150	150	150	150	150	150	150	150	150	150	150	150	150	150
	160	160	160	160	160	160	160	160	160	160	160	160	160	160	160	160
	170	170	170	170	170	170	170	170	170	170	170	170	170	170	170	170

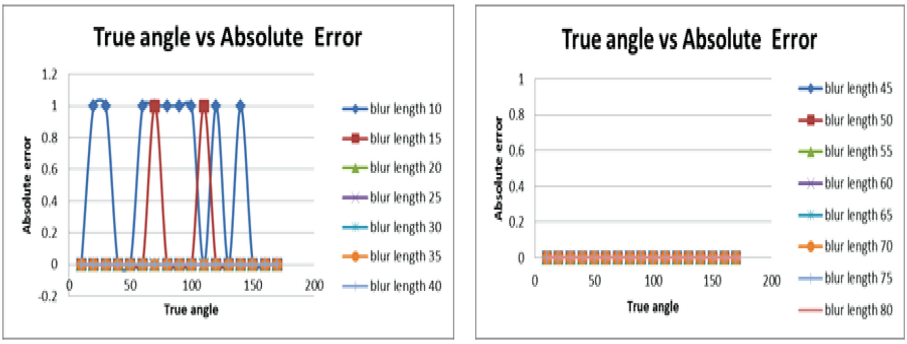

(a) (b)

Fig. 6. (a) True angle vs absolute error for blur length 10 to 40 pixels (b) True angle vs absolute error for blur length 45 to 80 pixels

5 Conclusion

Comparative analysis of PSF parameters estimation is shown in the paper concentrate on vital parameters like wide variation of blur extent and increasing accuracy of PSF estimation. The discussed PSF estimation is done in modified cepstrum domain using Hough transform and radon transform. Comparative analysis shows that even though Hough transform is flexible to use in case of broken line segments its PSF estimation accuracy is lower compare to radon transform based approach in large blur parameter variation range. Experimental results show that radon transform based approach is more accurate for wider variation of blur extent.

References

1. Gonzalez, R., Woods, R., Eddins, S.: Digital Image Processing Using MATLAB. Pearson Prentice-Hall, Upper Saddle River (2004)
2. Wang, R., Tao, D.: Recent progress in image deblurring. arXiv preprint arXiv:1409.6838 (2014)
3. Fergus, R., et al.: Removing camera shake from a single photograph. ACM Trans. Graph. **25**(3), 787–794 (2006)
4. Krishnan, D., Tay, T., Fergus, R.: Blind deconvolution using a normalized sparsity measure. In: CVPR (2011)
5. Xu, L., Zheng, S., Jia, J.: Unnatural L0 sparse representation for natural image deblurring. In: CVPR (2013)
6. Cho, J., Lee, S.: Fast motion deblurring. ACM Trans. Graph. **28**(5), December 2009
7. Sun, L., Cho, S., Wang, J., Hays, J.: Edge-based blur kernel estimation using patch priors. In: ICCP (2013)
8. Groetsch, C.W.: The Theory of Tikhonov Regularization for Fredholm Equations of the First Kind. Pitman, London (1984)
9. Osher, S., Burger, M., Goldfarb, D., Xu, J., Yin, W.: An iterative regularization method for total variation-based image restoration. SIAM Multiscale Model. Sim. **4**, 460–489 (2005)
10. Elad, M.: Sparse and Redundant Representations: From Theory to Applications in Signal and Image Processing. Springer, Heidelberg (2010)
11. Gennery, D.B.: Determination of optical transfer function by inspection of frequency domain plot. J. Opt. Soc. Am. **63**(12), 1571–1577 (1973)
12. Lokhande, R., Arya, K.V., Gupta, P.: Identification of parameters and restoration of motion blur images. In: ACM Symposium on Applied Computing, pp. 301–305 (2006)
13. Cannon, P.: Blind deconvolution of spatially invariant image blurs with phase. IEEE Trans. Acoust. Speech Sign. Process. **24**(1), 56–63 (1976)
14. Chen, C.H., Rui, Z.: Image restoration for linear local motion blur based on cepsturm. In: International Conference on Genetic and Evolutionary Computing (2012)
15. Park, J., Kim, M., Chang, S., Lee, K.H.: Estimation of motion blur parameters using cepstrum analysis. In: IEEE 15th International Symposium on Consumer Electronics (ISCE), pp. 406–409 (2011)
16. Deshpande, A.M., Patnaik, S.: A novel modified cepstral based technique for blind estimation of motion blur. Int. J. Light Electron. Opt. **125**(2), 606–661 (2014)

17. Agrawal, A., Xu, Y.: Coded exposure deblurring: optimized codes for PSF estimation and invertibility. In: IEEE Conference on Computer Vision and Pattern Recognition, New York, pp. 2066–2073 (2009)
18. Zhou, Y., Lin, S., Nayar, S.K.: Coded aperture pairs for depth from defocus and defocus deblurring. Int. J. Comput. Vis. **93**(1), 53–72 (2011)
19. Levin, A., et al.: Image and depth from a conventional camera with a coded aperture. ACM Trans. Graph. **26**(3) (2007)
20. Veeraraghavan, A., et al.: Dappled photography: mask enhanced cameras for heterodyned light fields and coded aperture refocusing. ACM Trans. Graph. **26**(3), July 2007
21. Hiura, S., Matsuyama, T.: Depth measurement by the multi-focus camera. In: Proceedings of IEEE Computer Society Conference on Computer Vision and Pattern Recognition, pp. 953–959 (1998)
22. Ben-Ezra, M., Nayar, S.K.: Motion-based motion deblurring. IEEE Trans. Pattern Anal. Mach. Intell. **26**(6), 689–698 (2004)
23. Shah, M.J., Dalal, U.: Blind estimation of motion blur kernel parameters using cepstral domain and Hough transform. In: Fifth International Conference on Advances in Computing, Communication and Informatics – ICACCI (2014)
24. Shah, M.J., Dalal, U.: Hough transform and cepstrum based estimation of spatial-invariant and variant motion blur parameters. In: International Conference on Advances in Electronics, Computers and Communications (ICAECC) (2014)